1
Reservoir Definition

Patrick Ledru and Laurent Guillou Frottier

1.1
Expressions of Earth's Heat Sources

1.1.1
Introduction to Earth's Heat and Geothermics

Scientific background concerning the heat flow and the geothermal activity of the earth is of fundamental interest. It is established that plate tectonics and activities along plate margins are controlled by thermal processes responsible for density contrasts and changes in rheology. Thus, any attempt to better understand the earth's thermal budget contributes to the knowledge of the global dynamics of the planet. Information on the sources and expressions of heat on earth since its formation can be deduced from combined analyses of seismic studies with mineral physics, chemical composition of primitive materials (chondrites), as well as pressure–temperature–time paths reconstituted from mineralogical assemblages in past and eroded orogens.

Knowledge of heat transfer processes within the earth has greatly improved our understanding of global geodynamics. Variations of surface heat flow above the ocean floor has provided additional evidence for seafloor spreading (Parsons and McKenzie, 1978), and improved theoretical models of heat conduction within oceanic plates or continental crust helped to constrain mantle dynamics (Sclater, Jaupart, and Galson, 1980; Jaupart and Parsons, 1985). When deeper heat transfer processes are considered, thermal convection models explain a number of geophysical and geochemical observations (Schubert, Turcotte, and Olson, 2002). It must be, however, noted that at a smaller scale (closer to the objective of this chapter), say within the few kilometers of the subsurface where water is much more present than at depths, a number of geological and geothermal observations are not well understood. As emphasized by Elder (1981), crustal geothermal systems may appear as liquid- or vapor-dominated systems, where physics of water–rock interactions greatly differs from one case to the other. Actually, as soon as hydrothermal convection arises among the active heat transfer processes, everything goes faster since heat exchanges are more efficient than without circulating water.

Geothermal Energy Systems. Edited by Ernst Huenges

ISBN: 978-3-527-40831-3

It is thus important to delineate which type of heat transfer process is dominant when geothermal applications are considered. Examples of diverse geothermal systems are given below.

Within the continental crust, a given heat source can be maintained for distinct time periods according to the associated geological system. Hydrothermal fields seem to be active within a temporal window around 10^4–10^5 years (Cathles, 1977), whereas a magma reservoir would stay at high temperatures 10–100 times longer (Burov, Jaupart, and Guillou-Frottier, 2003). When radiogenic heat production is considered, half-lives of significant radioactive elements imply timescales up to 10^9 years (Turcotte and Schubert, 2002). At the lower limit, one can also invoke phase changes of specific minerals involving highly exothermic chemical reactions (e.g., sulfide oxidation and serpentinization) producing localized but significant heat excess over a short (10^3–10^4 years) period (Emmanuel and Berkowicz, 2006; Delescluse and Chamot-Rooke, 2008). Thus, description and understanding of all diverse expressions of earth's heat sources involve a large range of physical, chemical, and geological processes that enable the creation of geothermal reservoirs of distinct timescales.

Similarly, one can assign to earth' heat sources either a steady state or a transient nature. High heat producing (HHP) granites (e.g., in Australia, McLaren *et al.*, 2002) can be considered as permanent crustal heat sources, inducing heating of the surrounding rocks over a long time. Consequently, thermal regime around HHP granites exhibits higher temperatures than elsewhere, yielding promising areas for geothermal reservoirs. On the contrary, sedimentary basins where heat is extracted from thin aquifers may be considered as transient geothermal systems since cold water reinjection tends to decrease the exploitable heat potential within a few decades.

Finally, regardless of the studied geological system, and independent of the involved heat transfer mechanism, existence of geothermal systems is first conditioned by thermal regime of the surroundings, and thus by thermal boundary conditions affecting the bulk crust. Consequently, it is worth to understand and assess the whole range of thermal constraints on crustal rocks (physical properties as well as boundary conditions) in order to figure out how different heat transfer mechanisms could lead to generation of geothermal systems.

The following subsections present some generalities on earth' heat sources and losses in order to constrain thermal boundary conditions and thermal processes that prevail within the crust. Once crustal geotherms are physically constrained by the latter and by rock thermal properties, distinct causes for the genesis of thermal anomalies are discussed.

1.1.2
Cooling of the Core, Radiogenic Heat Production, and Mantle Cooling

The earth's core releases heat at the base of the mantle, through distinct mechanisms. Inner-core crystallization, secular cooling of the core, chemical

separation of the inner core, and possibly radiogenic heat generation within the core yield estimates of core heat loss ranging from 4 to 12 TW (Jaupart, Labrosse, and Mareschal, 2007). Precise determinations of ohmic dissipation and radiogenic heat production should improve this estimate. Independent studies based on core–mantle interactions tend to favor large values (Labrosse, 2002), while according to Roberts, Jones, and Calderwood (2003), ohmic dissipation in the earth's core would involve between 5 and 10 TW of heat loss across the core–mantle boundary. The averaged value of 8 TW (Jaupart, Labrosse, and Mareschal, 2007) is proposed in Figure 1.1.

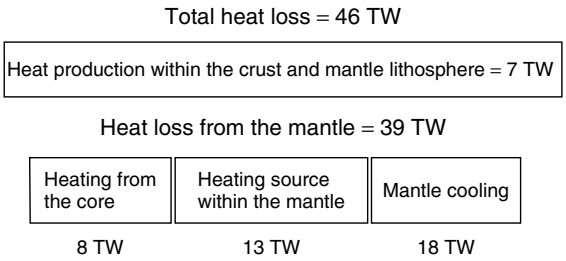

Figure 1.1 Heat sources and losses in the earth's core and mantle. (After Jaupart, Labrosse, and Mareschal, 2007.)

The earth's mantle releases heat at the base of the crust. Radiogenic heat production can be estimated through chemical analyses of either meteorites, considered as the starting material, or samples of present-day mantle rocks. Different methods have been used; the objective being to determine uranium, thorium, and potassium concentrations. Applying radioactive decay constants for these elements, the total rate of heat production for the bulk silicate earth (thus including the continental crust) equals 20 TW, among which 7 TW comes from the continental crust. Thus, heat production within the mantle amounts to 13 TW (Figure 1.1, Jaupart, Labrosse, and Mareschal, 2007). Since total heat loss from the mantle is larger than heat input from the core and heat generation within it, the remaining heat content stands for mantle cooling through earth's history.

Mantle cooling corresponds to the difference between total heat loss from the mantle (39 TW) and heat input (from the core, 8 TW) plus internal generation (13 TW). This 18 TW difference can be converted into an averaged mantle cooling of 120 $^{\circ}$C Gy^{-1}, but over long timescales, geological constraints favor lower values of about 50 $^{\circ}$C Gy^{-1}. Knowledge of the cooling rate enables one to draw a more accurate radial temperature profile through the earth (Jaupart, Labrosse, and Mareschal, 2007). However, as it is shown below, precise temperature profile within the deep earth does not necessarily constrain shallow temperature profiles within the continental crust.

1.1.3 Mantle Convection and Heat Loss beneath the Lithosphere

Heat from the mantle is released through the overlying lithosphere. Spatially averaged heat flow data over oceans and continents show a strong discrepancy between oceanic and continental mantle heat losses. Among the 46 TW of total heat loss, only 14 TW is released over continents. In terms of heat losses, two major differences between continental and oceanic lithospheres must be explained. First, oceanic lithosphere can be considered as a thermal boundary layer of the convective mantle since it does participate in convective motions. Actually, oceanic heat flow data show a similar decrease from mid-oceanic ridges to old subducting lithosphere as that deduced from theoretical heat flow variation from upwelling- to downwelling parts of a convecting system (Parsons and Sclater, 1977). Second, heat production within the oceanic lithosphere is negligible when compared to that of the continental lithosphere, enriched in radioactive elements. It follows that the oceanic lithosphere can be considered as a ''thermally inactive'' upper boundary layer of the convective mantle. In other words, the appropriate thermal boundary condition at the top of the oceanic mantle corresponds to a fixed temperature condition, which is indeed imposed by oceanic water.

Contrary to oceanic lithosphere, continental lithosphere is not directly subducted by mantle downwellings and behaves as a floating body of finite thermal conductivity overlying a convective system (Elder, 1967; Whitehead, 1976; Gurnis, 1988; Lenardic and Kaula, 1995; Guillou and Jaupart, 1995; Jaupart *et al.*, 1998; Grigné and Labrosse, 2001; Trubitsyn *et al.*, 2006). Even if atmospheric temperature can be considered as a fixed temperature condition at the top of continents, it does not apply to their bottom parts (i.e., at the subcontinental lithosphere–asthenosphere boundary) since heat production within continents create temperature differences at depths. Depending on crustal composition, heat production rates can vary from one continental province to the other, and lateral temperature variations at the conducting lithosphere–convecting asthenosphere boundary are thus expected. It follows that thermal boundary condition at the base of the continental lithosphere may be difficult to infer since thermal regime of continents differs from one case to the other. However, as it is suggested below, some large-scale trends in thermal behavior of continental masses can be drawn and thus a subcontinental thermal boundary condition may be inferred.

1.1.3.1 Mantle Heat Flow Variations

Since radiogenic heat production is negligible in oceanic lithosphere, heat flow through the ocean floor corresponds to mantle heat flow at the bottom of the oceanic lithosphere. This suboceanic heat flow varies from several hundreds of milliwatts per square meter at mid-oceanic ridges to about $50\,\mathrm{mW\,m^{-2}}$ over oceanic lithosphere older than 80 Myr (Lister *et al.*, 1990). When thermal effects of hydrothermal circulation are removed, this variation is well explained by the cooling plate model.

Beneath continents, mantle heat flow variations do not follow such simple physical consideration since large contrasts exist for both crustal heat production and lithospheric thickness. However, at the scale of the mantle, heat loss is mainly sensitive to large-scale thermal boundary conditions at the top of the convecting system, and not to the detailed thermal structures of the overlying lithospheres. Beneath continents, the earth's mantle is not constrained by a fixed temperature condition as is the case beneath oceanic lithosphere (see above), and thus large-scale temperature and heat flow variations are expected at the top surface of the subcontinental convecting system.

Surface heat flow measurements over continents and estimates of associated heat production rates have shown that mantle heat flow values beneath thermally stable (older than about 500 Myr) continental areas would be low, around $15 \pm 3\,\mathrm{mW\,m^{-2}}$ (Pinet *et al.*, 1991; Guillou *et al.*, 1994; Kukkonen and Peltonen, 1999; Mareschal *et al.*, 2000). On the contrary, mantle heat flow would be significantly enhanced beneath continental margins (Goutorbe, Lucazeau, and Bonneville, 2007; Lucazeau *et al.*, 2008) where crustal thickness and heat production rates decrease. Old central parts of continents would be associated with a low subcontinental mantle heat flow while younger continental edges would receive more heat from the mantle. The so-called ''insulating effect'' of continents is described here in terms of heat transfer from the mantle to the upper surface, where most of mantle heat flow is laterally evacuated toward continental margins and oceanic lithosphere. The term *insulating* should in fact be replaced by *blanketing* since thermal conductivity values of continental rocks are not lower than that of oceanic rocks (Clauser and Huenges, 1995).

1.1.3.2 **Subcontinental Thermal Boundary Condition**

A fixed temperature condition applies to the top of oceanic lithosphere while a low subcontinental heat flow is inferred from surface heat flow data over stable continental areas. As shown by laboratory experiments, this low mantle heat flow beneath continents cannot be sustained if continental size is small (Guillou and Jaupart, 1995). Indeed, a constant and low heat flux settles beneath a continental area for continental sizes larger than two mantle thicknesses. For smaller sizes, subcontinental heat flow is increased.

In the field, it was shown that mantle heat flow beneath stable continents may be as low as $10\,\mathrm{mW\,m^{-2}}$ (Guillou-Frottier *et al.*, 1995), whereas beneath continental margins, values around $50\,\mathrm{mW\,m^{-2}}$ have been proposed (Goutorbe, Lucazeau, and Bonneville, 2007; Lucazeau *et al.*, 2008). Beneath young perturbed areas, similar elevated values have been suggested, such as the mantle heat flow estimate of $60–70\,\mathrm{mW\,m^{-2}}$ beneath the French Massif Central (FMC) (Lucazeau, Vasseur, and Bayer, 1984).

At large scale, one may infer a continuous increase of mantle heat flow from continental centers to continental margins, but laboratory and numerical simulations of thermal interaction between a convecting mantle and an overlying conducting continent have shown that the mantle heat flow increase is mainly focused on

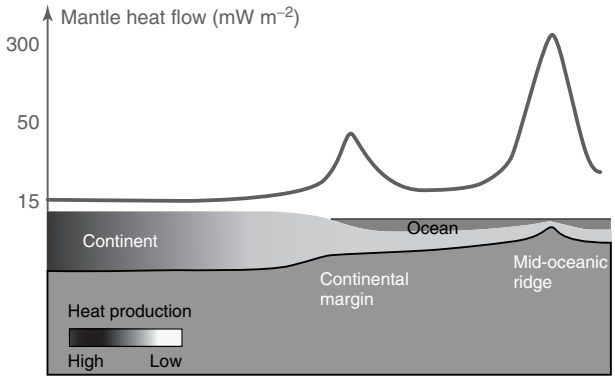

Figure 1.2 Sketch of mantle heat flow variations from continental center to mid-oceanic ridge, emphasizing a low subcontinental heat flow with a localized increase at continental margin, corresponding to a lateral decrease in crustal heat production.

continental margin areas (Lenardic *et al.*, 2000). In other words, the low and constant heat flow beneath the continent can be considered as the dominant large-scale thermal boundary condition applying above the subcontinental mantle (Figure 1.2).

1.1.4
Fourier' Law and Crustal Geotherms

Heat transfer within the continental crust occurs mainly through heat conduction. Heat advection may occur during magmatism episodes (arrival of hot magma at shallow depths enhancing local temperatures), intense erosion episodes (uplift of isotherms), and periods of hydrothermal convection. All these phenomena can be considered as short-lived processes when equilibrium thermal regime of the crust is considered. In steady state and without advective processes, the simplest form of Fourier law, with a constant thermal conductivity, a depth-dependent temperature field, and with appropriate boundary conditions for continental crust, can be written as

$$\begin{cases} k\left(\dfrac{\mathrm{d}^2T}{\mathrm{d}z^2}\right) + A = 0 \\ T(z=0) = T_0 \\ k\dfrac{\mathrm{d}T}{\mathrm{d}z}(z=h) = Q_\mathrm{m} \end{cases} \tag{1.1}$$

where k is the crustal thermal conductivity, A heat production, T_0 surface temperature, h the thickness of the crust, and Q_m the mantle heat flow. Temperature profile within the crust thus can be written as

$$T(z) = \frac{-A}{2k}z^2 + \frac{\left(Q_\mathrm{m} + Ah\right)}{k}z + T_0 \tag{1.2}$$

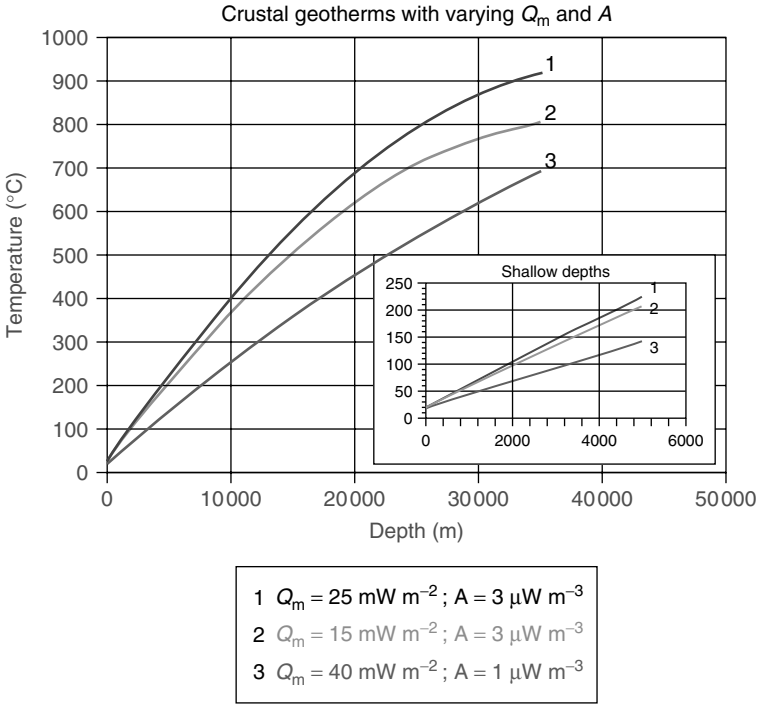

Figure 1.3 Synthetic simple temperature profiles as inferred from Equation 1.2, where mantle heat flow and bulk crustal heat production are varied.

This kind of geotherms show parabolic profiles where the curvature is controlled by A/k value. Temperature difference at depth greatly depends on both A and Q_m values. Figure 1.3 shows three crustal geotherms for a 35-km-thick crust, where surface temperature equals 20 °C, with an averaged thermal conductivity of 3 W m^{-1} K^{-1} and with different (A, Q_m) values.

As emphasized by curve 3 in Figure 1.3, a high mantle heat flow does not necessarily involve high crustal temperatures. Curvature of geotherms is indeed controlled by bulk heat production of the crust, as shown by curves 1 and 2. However, this curvature is not visible at shallow depths since the fixed temperature condition at the surface forces linear variation. These simple examples demonstrate that construction of crustal temperature profiles is strongly dependent on both estimates of mantle heat flow and of bulk crustal heat production.

At shallow depths, temperature anomalies may thus be due to anomalous HHP rocks. Likewise, other lateral heat transfer effects such as those due to thermal conductivity contrasts may lead to strong temperature differences at a given depth. In the following sections, a series of synthetic temperature profiles are built and discussed based on the geological examples.

1.1.5
Two-dimensional Effects of Crustal Heterogeneities on Temperature Profiles

1.1.5.1 Steady-state Heat Refraction

The two-dimensional heterogeneity of the upper crust is outlined by geological maps, where, for example, each rock composition is assigned one color. However, it must be emphasized that thermal properties are not necessarily correlated with rock composition, except for extreme cases (Clauser and Huenges, 1995). On one hand, one may record similar temperature profiles through distinct areas where small-scale lithological differences are observed, because the averaging effect of heterogeneities smoothes out small-scale variations. On the other hand, when large bodies with significantly distinct thermal properties are present, temperature profiles may differ by several tens of degrees at shallow depths. In other words, the horizontal geometry of anomalous bodies shall play a significant role in the establishment of temperature differences at depth.

As far as surface heat flow is concerned, small-scale lithological contrast may create large differences. For example, subvertical mineralized bodies can be rich in highly conducting minerals (e.g., volcanic massive sulfides deposits, Mwenifumbo, 1993), which may result in large surface heat flow variations, whereas

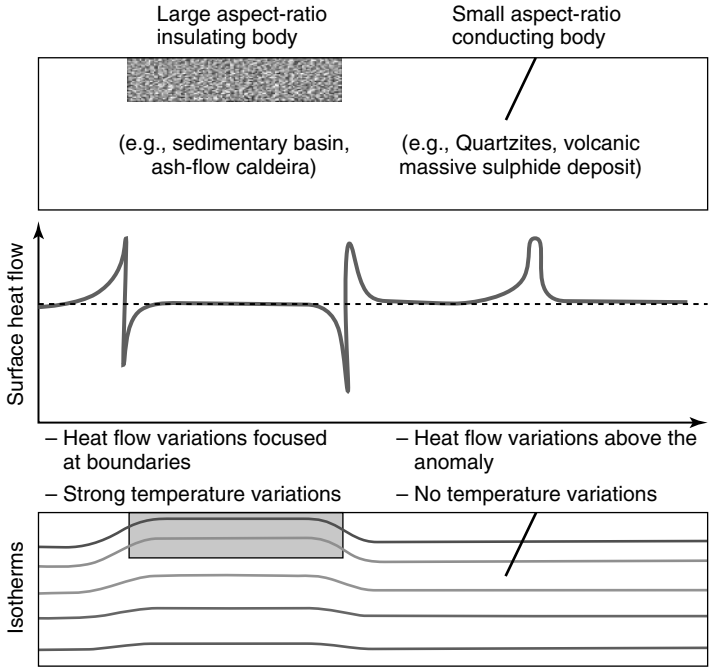

Figure 1.4 Heat refraction in two dimensions, leading to opposite effects according to the conductivity contrast or the anomaly geometry.

differences in subsurface temperatures may be negligible. These subtle effects are illustrated in Figure 1.4, where two scenarios of heat refraction effects are illustrated. The objective here is to show that high surface heat flow variations do not necessarily correlate with large subsurface temperature differences since geometrical effects have to be accounted for. Indeed, above a large aspect-ratio insulating body, isotherms are uplifted so that surface heat flow above the anomaly center corresponds to the equilibrium one. On the contrary, isotherms cannot be distorted for a small aspect-ratio conducting body but the resulting surface heat flow is enhanced.

In sedimentary basins, presence of salt may also induce heat refraction effects since thermal conductivity of halite may be four times greater than surrounding sediments (e.g., 1.5 W m^{-1} K^{-1} for sediments and around 6–7 W m^{-1} K^{-1} for rock salt and halite, according to Clauser, 2006). Consequently, temperature gradient within a thick evaporitic layer may thus be decreased by a factor of 4, leading to a cooling effect of several tens of degrees centigrade for a 2–3-km-thick layer.

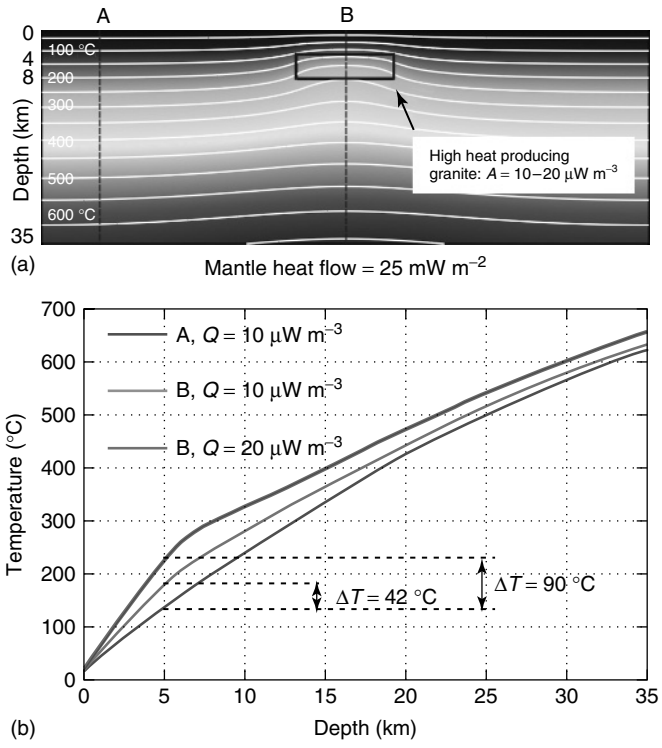

Figure 1.5 Two-dimensional effect of a high heat producing granite on temperature field (a) and geotherms (b). Here, a fixed mantle heat flow of 25 mW m^{-2} is imposed, as well as an averaged thermal conductivity of 3 W m^{-1} K^{-1} and a bulk crustal heat production of 1 μW m^{-3}.

Apart from thermal conductivity contrasts, heat production rates may also vary by a factor of 10 or more between two lithologies (Sandiford, McLaren, and Neumann, 2002; McLaren *et al.*, 2002). In the case of HHP granites, radiogenic content is so high that heat production rates may reach 10–20 $\mu W\ m^{-3}$, as it is the case of the synthetic example of Figure 1.5, where embeddings have an averaged heat production rate of 1 $\mu W\ m^{-3}$. At 5 km depth, a temperature difference of 42 °C (90 °C) is obtained for a high heat production of 10 (20) $\mu W\ m^{-3}$.

In the case of Figure 1.5, the obtained temperature anomaly depends on several other parameters such as the emplacement depth of the anomalous body. For example, same granite of Figure 1.5 emplaced at 10 km depth would involve a 30 °C anomaly at 5 km depth. This temperature difference also corresponds to the case of a shallow emplacement of 500 m below the surface. This nonobvious result can be explained by detailed analysis of geotherm curvature, as presented by Sandiford, Fredericksen, and Braun (2003).

1.1.5.2 **Transient Effects**

A number of studies have demonstrated the role of transient geological processes on crustal temperatures. Large-scale tectonic processes (thrusting events, erosion, and sedimentation) can result in temperature differences reaching several tens of degrees centigrade at a few kilometers depth (England and Thompson, 1984; Ruppel and Hodges, 1994). Magma emplacement or presence of hydrothermal convection at shallow depths may also explain disturbed temperature profiles (Cathles, 1977; Norton and Hulen, 2001).

Because thermal diffusivity of rocks is low, transient thermal evolution of rocks undergoing conducting processes is very slow, and return to equilibrium temperatures may last several tens to hundreds of million years. Figure 1.6 illustrates some examples of large-scale thermal evolution of the crust undergoing tectonic events. One may note that in the case of a thrusting event, the equilibrium thermal field (with a maximum temperature of 820 °C) is reached 120 Myr after the onset of thrusting. On the contrary, when convective processes are involved around intrusive bodies, heat transfer mechanisms through fluid circulation are accelerated, and typical timescales are lower than 1 Myr (Cathles, 1977). When smaller scale systems are considered, thermal equilibrium is reached faster. For example, serpentinization of oceanic crust may result in large amplitude thermal signatures lasting less than a few thousands of years (Emmanuel and Berkowicz, 2006).

1.1.5.3 **Role of Anisotropy of Thermal Conductivity**

Apart from steady-state heat refraction due to thermal conductivity contrasts or variations in heat production rates, other subtle effects affecting thermal properties may trigger thermal anomalies. Temperature dependence of thermal conductivity is one example, as shown in Clauser and Huenges (1995). In the case of sedimentary basins, porosity dependence of thermal conductivity is also significant, as shown in several studies (Beziat, Dardaine, and Gabis, 1988; Waples and Tirsgaard, 2002). Sedimentary basins correspond to interesting geothermal targets all the more that numerous temperature measurements may be available. When thick clayey

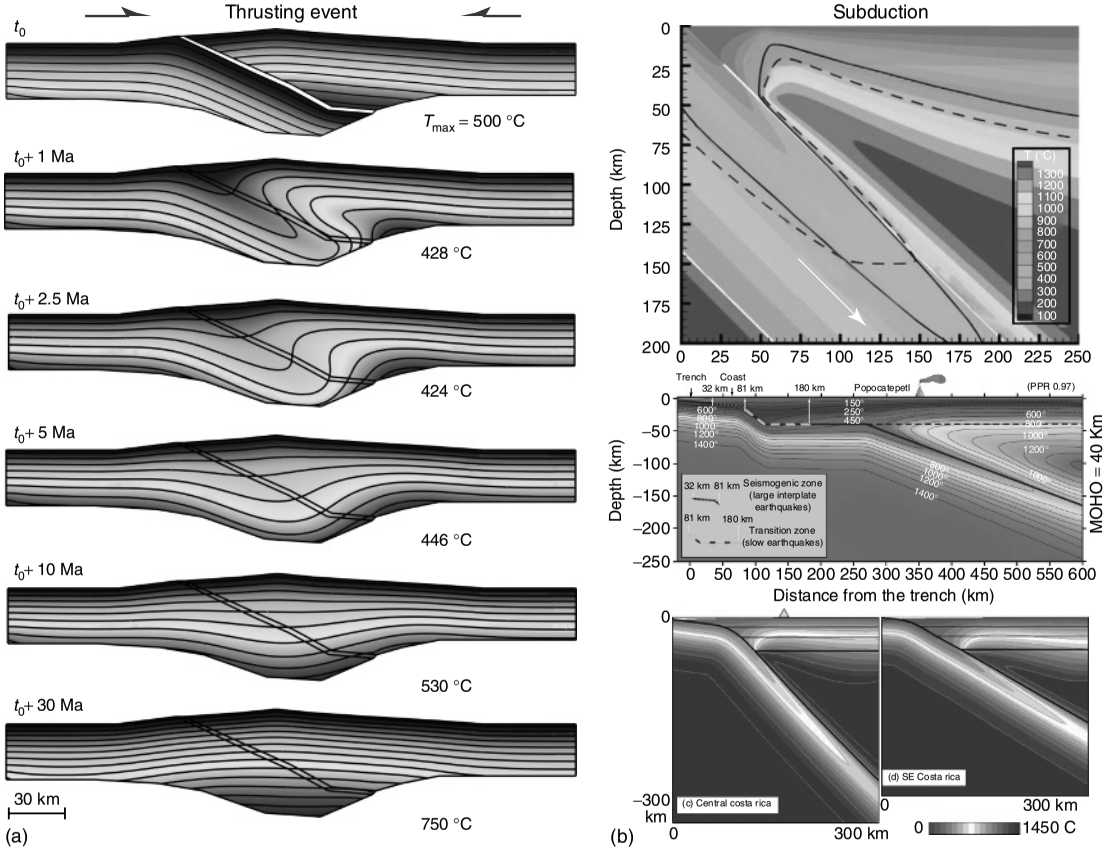

Figure 1.6 Examples of large-scale transient and steady-state thermal perturbations: (a) thrusting event resulting in a thickened and more radiogenic crust and (b) distinct models of thermal fields around subduction zones, where slab dip angle and plate velocities differ from one case to the other. (After, from top to bottom, Cagnioncle, Parmentier, and Elkins-Tanton, 2007; Manea *et al.*, 2004; Peacock *et al.*, 2005.) (Please find a color version of this figure on the color plates.)

formations are present in a basin, the role of compaction has to be accounted for since porosity decreases with compaction pressure and particles' orientation becomes horizontal with increasing pressure (Vasseur, Brigaud, and Demongodin, 1995). Both effects together with temperature-dependence effect induce important changes in thermal conductivity. First, the decreasing porosity (and thus amount of water) with depth tends to increase thermal conductivity, while temperature dependence tends to decrease it (see Harcouët *et al.*, 2007 for details). Second, the horizontal orientation of individual clay particles develops anisotropy, favoring lateral heat transfer and hindering vertical heat flow.

An example of the effect of thermal conductivity anisotropy on thermal field is illustrated in Figure 1.7, where the Paris basin is modeled according to Demongodin *et al.* study (1991)). Anisotropy ratio is increased with depth and thermal boundary conditions enable to reproduce measured surface heat flow values. Figure 1.8b shows horizontal temperature profiles at 1500 m depth, with and without anisotropy effect. When anisotropy is accounted for, heat accumulates more efficiently within the basin and a 20 °C difference with the isotropic case is reached at basin boundaries. Obviously, the importance of the anomaly critically depends on thermal conductivity values and anisotropy ratios. Measurements on representative core samples, and scaling with *in situ* conditions are thus of major importance when thermal modeling of a sedimentary basin is performed (Gallagher *et al.*, 1997).

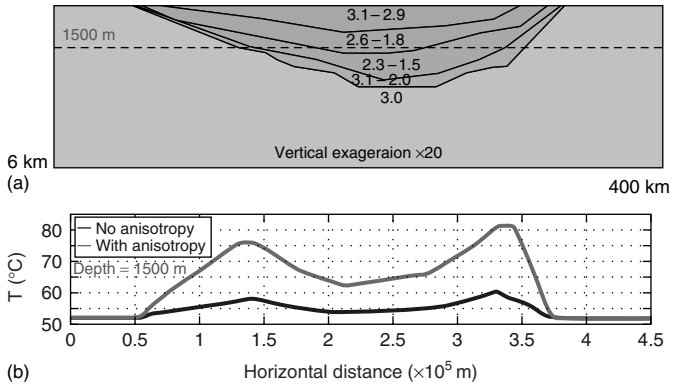

Figure 1.7 (a) Chosen model for the Paris basin (after Demongodin *et al.*, 1991), with thermal conductivity values indicated as follows: ''horizontal component–vertical component.'' When anisotropy is not accounted for, the first value is considered as homogeneous. (b) Horizontal temperature profiles at 1500 m depth across the basin (see text).

1.1.6
Fluid Circulation and Associated Thermal Anomalies

In previous sections, heat transfer was described by pure conduction, where no heat transfer by fluid motion could occur. However, shallow geological systems are sometimes characterized by sufficiently porous layers (sedimentary units) or

highly permeable areas (fault zones) in which crustal fluids may freely circulate. Depending on fluid velocity, permeability, or thickness of the porous layer, heat from several kilometers depth may be entrained by fluid circulation and thus create temperature anomalies.

Several studies have demonstrated the possibility to detect fluid motion by temperature measurements within boreholes (Drury, Jessop, and Lewis, 1984; Pribnow and Schellschmidt, 2000). Small-scale water flows through a fracture crossing the borehole may disturb locally the measured geotherm by a few degrees centigrade (Vasseur *et al.*, 1991), and large-scale fluid circulation (convective flows) may lead to cooling or warming effects exceeding tens of degrees centigrade (Lopez and Smith, 1995; Bächler, Kohl, and Rybach, 2003; Wisian and Blackwell, 2004). In some cases, the measured temperature anomalies cannot be explained by purely conductive processes and one must account for free convection in highly permeable fault zones (Rühaak, 2009; Garibaldi *et al.*, 2010).

1.1.7
Summary

Crustal temperatures are controlled by thermal boundary conditions and thermal properties of rocks. In the pure conductive regime, knowledge of mantle heat flow and crustal heat production enables to determine a probable averaged geotherm, but the natural heterogeneity of crustal composition may lead to local variations reaching several tens of degrees centigrade at a few kilometers depth. When available thermal data are used to infer deep temperatures (as it is the case in the next section), similar uncertainties can be assigned to extrapolated data.

Despite the fact that crustal temperatures are not easy to estimate, it is shown in Section 1.1 that models of geothermal reservoirs depend on several other parameters, which may be less constrained than thermal properties. In particular, the presence of fluids, which is important in the development of geothermal energy, may completely distort temperature field as soon as rock permeability is high enough (Manning and Ingebritsen, 1999). Within sedimentary basins, permeability can vary by approximately four orders of magnitude, thus allowing or preventing fluid circulation. The detailed knowledge of temperature field in an area is probably not sufficient to characterize a geothermal reservoir.

Before defining the concept of geothermal reservoir, heat flow data from Europe are reviewed and presented. The objective of this second section is to illustrate how surface heat flow and deep temperatures are not necessarily correlated, and how significant errors in deep temperature estimates can be made when shallow measurements are extrapolated at depth.

1.2
Heat Flow and Deep Temperatures in Europe

Independent of numerical modeling of heat transfer within geological systems, the best way to search for thermal anomalies in the shallow crust consists first

in compiling available thermal data that correspond to the boundary conditions, as well as petrophysical parameters controlling heat transfer. Surface temperature is well known, but may however show significant spatial variations as detailed below. The few direct measurements of surface heat flow in Europe are also shown together with temperature gradients and thermal conductivity values. At mantle depths, indirect evidence for temperature variations in Europe has been evidenced.

1.2.1 Far-field Conditions

In order to constrain thermal regime of the shallow crust, one need to constrain far-field thermal boundary conditions, say at the surface and at the base of the lithosphere. Even if spatial distribution of heat producing elements within the crust is of major importance, it is necessary to estimate the amount of heat supplied at the base of the lithosphere (which is also the heat supplied at the base of the crust) and that lost at the surface.

At the surface, the ground surface temperature has been measured for centuries and can be considered as constant over length scales of several hundreds of kilometers (Hansen and Lebedeff, 1987). In Europe, ground surface temperature increases from north to south France (~1000 km) by about 5 °C, and by ~10 °C from Denmark to south Italy (Figure 1.8) separated by a distance of 2000 km (Haenel *et al.*, 1980). If thermal regime of the crust is to be studied, such large-scale variations can thus be neglected. Apart from the effect of latitude, ground surface temperature can be locally disturbed by surface heterogeneities such as topography (Blackwell, Steele, and Brott, 1980) or the presence of lakes. These permanent disturbances should be theoretically considered when subsurface temperatures are studied, especially if representative length scale of surface features compare with the studied depths (e.g., warm water outflows in tunnels of Switzerland, Sonney and Vuataz, 2008). Transient changes in surface conditions such as those induced by forest fires may also affect subsurface temperatures but only for a short period. Long-period surface temperature changes such as climatic warming or cooling periods affect underground temperatures as it can be deciphered through measured temperature profiles (Guillou-Frottier, Mareschal, and Musset, 1998), but associated thermal disturbances are damped with depth, and basically cancelled at several hundreds of meters.

Contrary to the upper surface, there is no reason to consider the base of the crust as an isotherm. Seismic tomography studies have indicated that this is indeed not the case. Even if seismic velocities vary with temperature and composition, Goes *et al.* (2000) suggested that the inferred variations at 100 km depth revealed temperature differences (Figure 1.8). At shallower depths (Moho depth +20 km), Figure 1.9 shows possible large-scale temperature differences as deduced from the shear velocity model of Shapiro and Ritzwoller (2002). Local studies of seismic tomography also suggested anomalous hot zones at the base of the European crust, such as beneath the FMC and beneath the Eifel area in Germany (Granet, Wilson, and Achauer, 1995; Ritter *et al.*, 2001). These anomalously hot zones and

Figure 1.8 Mean annual surface (air) temperature (in degrees centigrade) in Western Europe as published in Haenel *et al.* (1980), after a Climatic Atlas published in 1970 by UNESCO.

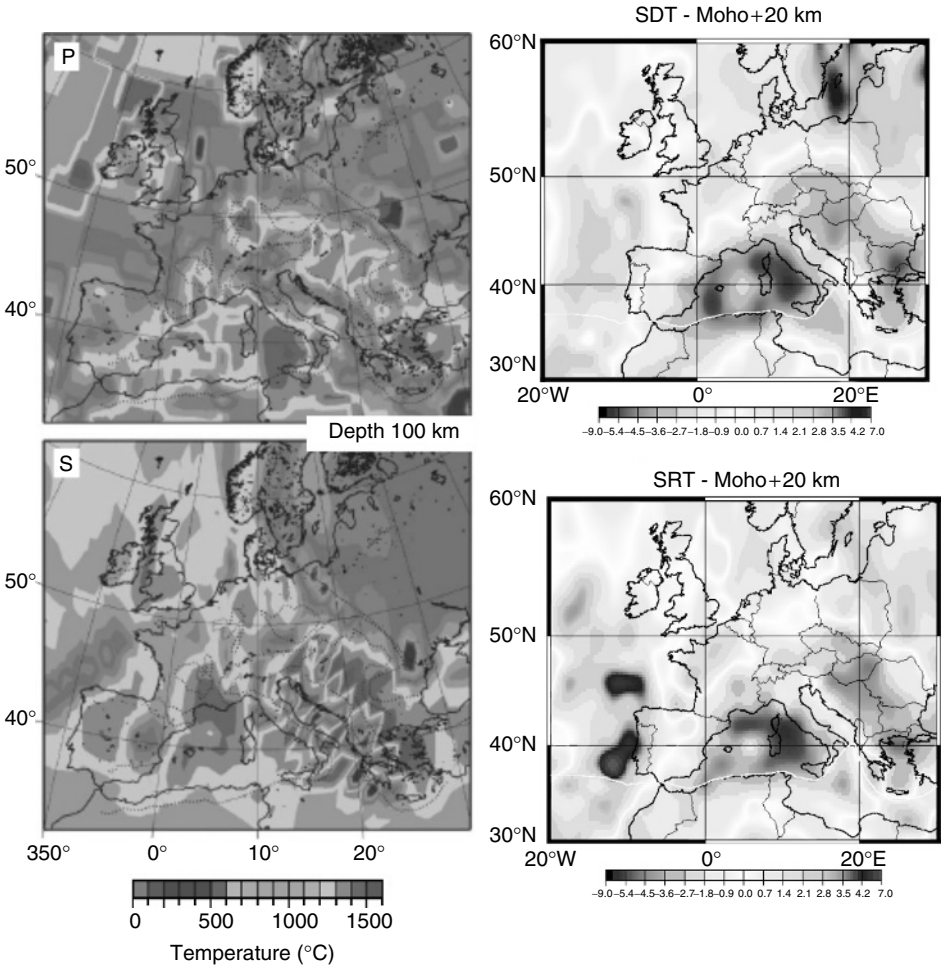

Figure 1.9 Left: Temperatures at 100 km depth estimated from the P and S velocity anomalies. (After Goes *et al*., 2000.) Right: Tomographic models extracted from an upper mantle shear velocity model (Shapiro and Ritzwoller, 2002); top: diffraction tomography, bottom: ray tomography. (Please find a color version of this figure on the color plates.)

their surface signatures would be associated with local mantle upwellings (Goes, Spakman, and Bijwaard, 1999; Guillou-Frottier *et al*., 2007), thus reinforcing the possible increase in underlying heat flow. For the FMC area, Lucazeau, Vasseur, and Bayer (1984) used distinct geophysical data to build a thermal model and concluded that an additional heat flow contribution from the mantle of 25–30 mW m^{-2} can explain surface heat flow data. While a mantle heat flow of 40 mW m^{-2} is present in the vicinity of the FMC, it would locally reach 70 mW m^{-2} beneath parts of the FMC where a thin crust is seismically detected.

1.2.2
Thermal Conductivity, Temperature Gradient, and Heat Flow Density in Europe

The global heat flow database (International Heat Flow Commission, IHFC; http://www.heatflow.und.edu) contains almost all published heat flow measurements that were available at the time of its publication (Cermak, 1993; Pollack, Hurter, and Johnson, 1993). Each heat flow data is provided with supplementary information such as thermal conductivity, heat production rates, and temperature gradients that were used to estimate surface heat flow. However, there is no information on data quality, which depends on several independent factors (precision of measurements, depth of boreholes, stability of temperature gradient, etc.). In order to improve the IHFC database quality, the few new published thermal data in Europe have been added (Cermak *et al.*, 1996; Nemcock *et al.*, 1998; Demetrescu and Andreescu, 1994; Aydin, Karat, and Kocak, 2005), related data have been clustered, and a quality criterion has been applied. In addition, numerous anomalous values have been removed (e.g., those lower than 25 mW m^{-2}). Because the quality criterion accounts for the number of individual boreholes used, data close to each other (separated by less than 15 km) have been affected a single mean value. The quality criterion accounts for (i) the number of individual boreholes used for heat flow estimate, (ii) the standard deviation of the estimate (s.d. in Table 1.1); (iii) the minimal depth where temperature measurements are accounted for; and (iv) the depth range where estimate is performed. These last two criteria enable to retain only stable and undisturbed temperature profiles for heat flow estimates. High, medium, and low quality criteria are detailed in Table 1.1.

This process of data treatment provided 1643 heat flow data, whereas 3520 original data were present in the IHFC database. More than 1000 data from Russia had to be removed or were clustered with neighboring ones. In Austria, the hundreds of data presented by Nemcock *et al.* (1998) decreased to 36 of quality 3. Numerous heat flow data in the IHFC database are deduced from individual

Table 1.1 Quality criteria assigned to heat flow data shown in Figure 1.10.

Site characteristics	Quality[a]
Several boreholes, good s.d. (<10%), depth range of estimate >200 m	1
Several boreholes, good s.d. (<10%), unknown or shallow (<200 m) depth range	2
Several boreholes, medium s.d. (between 10 and 30%), depth range >200 m	2
Several boreholes, medium s.d. (between 10 and 30%), unknown or shallow (<200 m) depth range	3
Several boreholes, bad s.d. (>30%)	3
One borehole, depth range >200 m	2
One borehole, depth range <200 m	3

[a]When one major information is missing (temperature gradient or thermal conductivity), then quality is decreased by one unit.

measurements where temperature gradient or thermal conductivity is not indicated, thus involving removal of the data. At last, a total of 257 data of high quality, 869 of medium quality, and 517 of low quality were obtained. Figure 1.10 illustrates the newly obtained heat flow map together with thermal conductivity and temperature gradient values.

Figure 1.10 does not present any contours of thermal data, which are simply gathered according to their range of values. Indeed, as previously indicated, there are many reasons to explain short-scale variations in temperature gradient and heat flow data. It is thus somehow dangerous to assign a given thermal regime in a geological area since even lithological changes may lead to significant local variations. In addition, one can see that thermal conductivity data appear surprisingly constant in some areas (Ukraine, Belorussia), revealing that the same value was probably assumed for tens of boreholes. These maps also indicate that heat flow values are sometimes estimated with no thermal conductivity data (e.g., Spain).

1.2.3
Calculating Extrapolated Temperature at Depth

Temperature measurements in mining or petroleum boreholes were used in the last decades to construct temperature maps at different depth levels (Haenel *et al.*, 1980; Hurtig *et al.*, 1992). Bottomhole temperature (BHT) measurements in petroleum boreholes are not necessarily representative of the equilibrium temperatures, and some corrections are needed (Goutorbe, Lucazeau, and Bonneville, 2007). However, because of the lack of information, a statistical method is often used to infer possible equilibrium temperatures. When temporal history of BHT measurements is well documented, appropriate corrections for transient disturbances can yield temperature estimates at a few kilometers depth with uncertainties of $\pm 10\,^{\circ}C$ (Bonté *et al.*, 2010).

In the last decade, the extrapolation of European temperatures to 5 km depth was performed by petroleum industry using such BHT measurements (which are unavailable), and where any uncertainty propagates and increases with depth through a linear extrapolation. This map was reviewed and analyzed by Genter *et al.* (2003). Using the deepest equilibrium temperature gradients inferred from measurements in mining boreholes (present in the IHFC database) and from recent studies (Fernàndez *et al.*, 1998), the authors performed a critical analysis of the temperature map presented by Hurtig *et al.* (1992), which was then modified by the ''heat mining Economic Interest European Group'' but only available as an unpublished map. Results of color validation are shown in Figure 1.11. It must be emphasized that the objective of this work was simply to use available thermal data to check the interest of some areas which was deduced from confidential data. When one color code is not confirmed, a temperature difference greater than $20\,^{\circ}C$ is obtained. When it is partly confirmed, it means that extrapolations are coherent for only a restricted area. The analysis

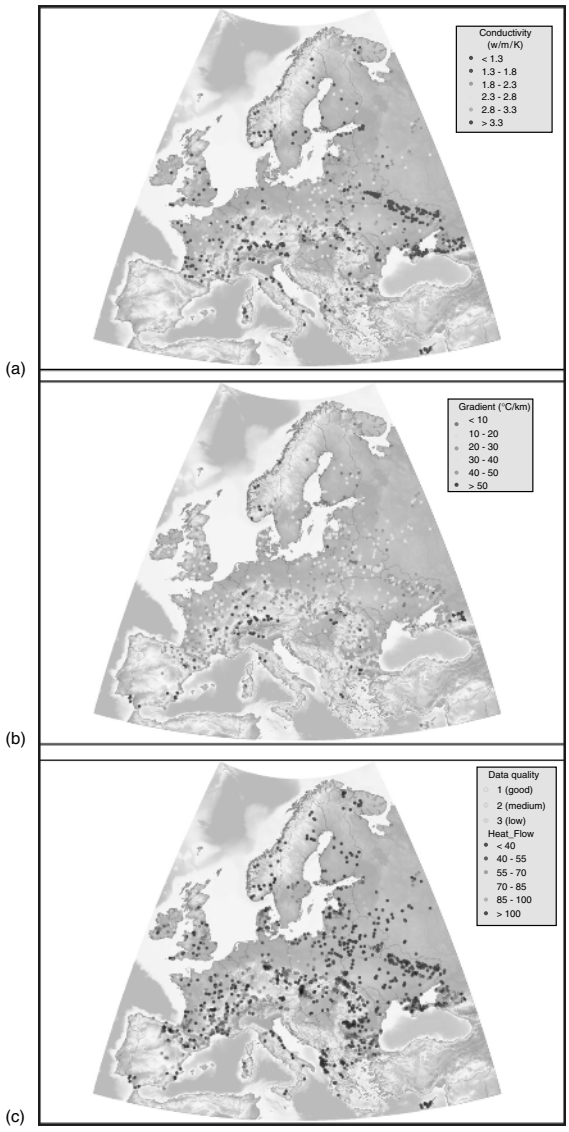

Figure 1.10 Thermal conductivity (a), temperature gradient (b), and heat flow data (c) as compiled from this study. Each color is assigned a range of values, and for heat flow data, a quality criterion is added (see text). (Please find a color version of this figure on the color plates.)

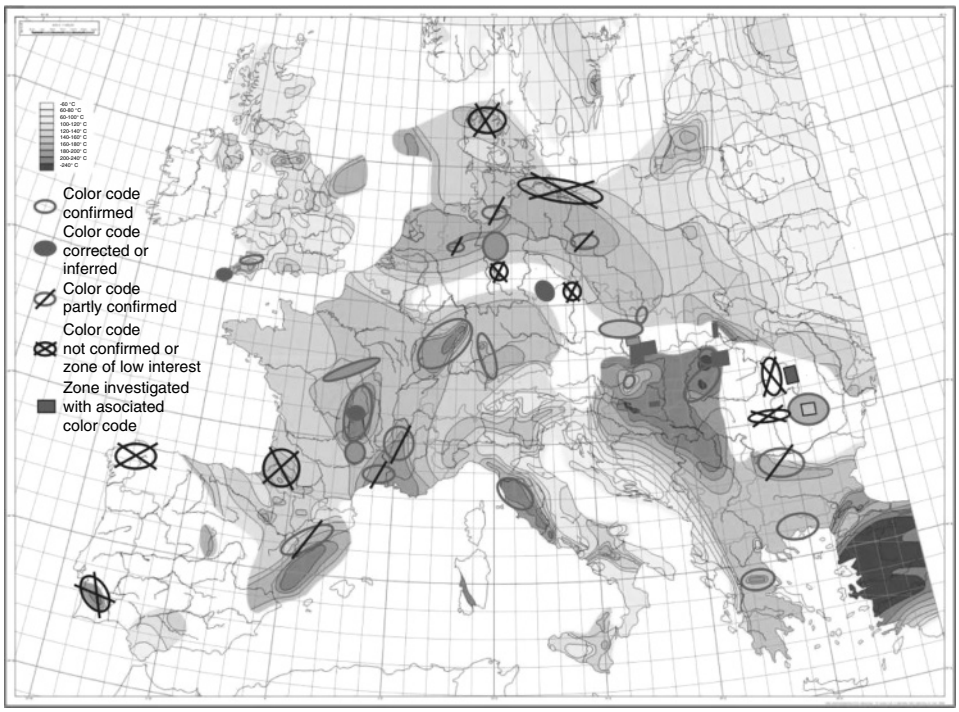

Figure 1.11 Map of temperature at 5 km depth, as inferred from unavailable (confidential) BHT measurements (Hurtig *et al*., 1992; EIEG, 2000) and critical analysis by Genter *et al*. (2003) from published thermal data (see text). (Please find a color version of this figure on the color plates.)

was not exhaustive but it shows that differences of several tens of degrees centigrade at 5 km depth may be easily reached when two extrapolation methods are investigated.

1.2.4 Summary

These different data sets were used for a predictive survey to evaluate potential zones of high heat flow where enhanced geothermal systems could be experimented. This approach takes only the thermal aspect of the geothermal systems into account without any geological a priori. At the scale of Europe (Figure 1.11), it reveals large wavelength positive anomalies in Italy, Central-Eastern Europe, and Turkey, which correspond to well-known geothermal systems located in extensional settings within active geodynamic systems and to which Iceland could be associated although it is not represented on the map.

In Italy, since Miocene, the Northern Apennine fold belt has been progressively thinned, heated, and intruded by mafic magmas. In Tuscany, this evolution is

the source of a granitic complex that has been emplaced between 3.8 and 1.3 Ma. A long-lived hydrothermal activity is recorded in this area by both fossil (Plio-Quaternary ore deposits) and active (Larderello geothermal field) systems (Dini *et al.*, 2004). In Central-Eastern Europe, the Pannonian basin is characterized since Middle Miocene by an upwelling of the asthenosphere and thinning of the lithosphere, responsible for coeval rifting in the basin and compression in the flanking Carpathian and Dinaric belts (Huismans, Podladchikov, and Cloetingh, 2001). In Turkey, the collision between the Arabian and Eurasion plates has induced the westward escape of the Anatolian block, which is accommodated by the right-lateral movement of the Anatolian fault network. Much of the geothermal activity appears to be focused along kinematically linked normal and strike-slip fault systems most commonly within E-W-trending grabens (Sengör, Gorur, and Saroglu, 1985; Ercan, 2002).

Besides these active tectonic zones, other positive anomalies are mainly distributed along a series of intracontinental grabens that cut the western European platform, corresponding to the west European rift system (Dèzes, Schmid, and Ziegler, 2004). These rift structures, the upper Rhine graben, the Limagne system, the Rhône valley, a part of Provence, the Catalonia, and the Eger grabens, were created in the Oligocene as a result of the thinning of the continental crust. Among these structures, the Rhine graben has been intensively studied over the last 10 years for its potential. It is about 300 km long, with an average width of 40 km, limited by large-scale normal faults. The post-Paleozoic sediments of the western European platform have overlain the Hercynian basement, which is made of granite, granodiorite, or other related basement rocks (Edel and Fluck, 1989). This area – characterized by a thin continental crust and a Moho at 25 km depth – shows a Tertiary volcanism that occurred in the form of isolated volcanoes of alkaline composition related to a mantle magmatic activity (Wenzel and Brun, 1991).

This preliminary analysis shows that the thermal aspect of the geothermal systems is directly linked and controlled by the past and present geodynamic context. This framework provides a first-order constrain on the location of favorable and unfavorable geodynamic sites for the exploration of potential geothermal reservoirs. In order to define conceptual models, these different contexts will be reviewed and complemented by an evaluation of the main properties of the potential reservoir in terms of porosity, permeability, fluid flow with respect to the stress field.

1.3
Conceptual Models of Geothermal Reservoirs

From a geological point of view, geothermal reservoirs are heated and pressurized water and/or vapor accumulations from which heat can be extracted from the underground to the surface. From a technical, environmental, and economic approach, the geothermal reservoir can be defined by the cost-efficiency of this extraction depending on the temperature, depth and size of the accumulation, the fluid flow, and the industrial process under which it will be processed. Although

this approach is highly dependent on economical indicators that are not linked to geology (price of energy, incentives politics for access to renewable energies, etc.), reference to present-day parameters will be provided for the different types of reservoirs.

1.3.1 The Geology of Potential Heat Sources

To get heat is the first condition for defining a geothermal reservoir. How can we explore potential heat sources? It has been shown that thermal boundary conditions (the mean annual surface temperature, temperatures at depth estimated from the P and S velocity anomalies) and thermal properties of the main lithologies and structure at depth enable the first calculation of extrapolated temperature at depth and thus the delineation of potential zones of high-thermal gradient.

Such zones can also be determined through a geological empiric approach. Heat is transferred within the crust through two mechanisms:

- The main active and permanent phenomenon at the scale of the continental crust is the conduction of heat. In conduction, heat moves through the material from a hotter to a cooler zone. The feasibility and intensity of such transfer is directly linked to the thermal properties of the mineral constituting the rock that is evaluated as the thermal conductivity. As continental crust is heterogeneous and a result of the superposition of layers with different conductivity properties (stacked allochthonous units over autochthonous cover sequence or basement in orogenic zones, sedimentary basins over basement within intracratonic zones, etc.), conduction will not be homogenous at the scale of the whole continental crust. Highly conductive zones such as fractured granites will be explored with interest while refractory units such as mafic units will be considered as potential thermal insulator.
- In convection, heat is transported by the movement of hot material. The ascent and emplacement of a granitic body or of a volcanic dyke network is a typical example of convection where heat is transferred from deep source and then dissipated by conduction in the host rocks at shallow level. Contact metamorphism is a direct expression of the elevation of temperature with respect to extreme geothermal gradients reaching 500 °C for granites emplaced at around 5 km depth. Globally, convection leads to anisotropic diffusion of heat; the movement of hot material being, most of the time, controlled by the permeability system of the continental crust, mainly fracture network.

The past or present geodynamic context gives a first-order constrain on the location of favorable and unfavorable geodynamic sites for high geothermal gradients. Conduction is directly controlled by the thickness, heterogeneity, and composition of the continental crust, whereas convection processes are mainly located within active zones of magmatism and metamorphism.

Rift in accretionary systems are characterized by thinned crust and lithosphere, in relation with asthenospheric doming and upwelling. This definition covers both

mid-oceanic ridges and back arc extensional systems, immerged or emerged, and to less extent pulls part systems developed along strike-slip faults. The geological setting of such rift zones is then the most favorable context because of the high mantle heat flow (Figure 1.2), the shallow depth of the mantle crust boundary, and the periodic magmatic activity (emplacement of stocks, sills, and dykes) and volcanic flow of hot mafic lavas. Moreover, convection of heat is enhanced by fluid – rock interaction – intense fracturing related to extensional tectonics favoring exchange between fluids of superficial and deep origin in the vicinity of magma chambers. Numerical modeling of rifting processes illustrates the shift of the isotherms toward surface depending on rifting velocities, presence of strain softening, and time (Huismans and Beaumont, (2002), Figure 1.12).

Iceland is the best case history for illustrating this first-order parameter for location of high geothermal gradients (Figure 1.13). A large active volcanic zone, corresponding to the mid-oceanic ridge, is running SW–NE, and displays various heat sources (dikes and magma chambers). Seawater, meteoric water, and volcanic fluids are mixed in pressurized water-dominated reservoirs, often associated with young tectonic fractures, carrying heat from several kilometers depth toward the surface (Flóvenz and Saemundsson, 1993; Arnórsson, 1995). The regional temperature gradient varies from 50 to 150 °C km^{-1} and the highest values are found close to the volcanic rift zone.

Active margins related to subduction are sites of intense convection with respect to magmatic activity. A computed model at the scale of the lithosphere (Figure 1.6) shows that the subduction of cold lithosphere is accompanied by a raise of hot lithosphere just above the main plate boundary. Thus, large crustal zones have temperatures greater than 300 °C at very shallow depth and undergo melting conditions at few kilometers depth. Generated calc-alkaline magmatism is responsible for the intrusion of voluminous granitic suites at shallow depth and related volcanism of intermediate to felsitic composition. This convective phenomenon at the scale of the lithosphere is also responsible of the concentration of U, K, and Th radioelements in the upper crust, which will contribute to the thermal budget of the continents over a long period.

Active margin settings are zones with almost infinite source of fluids from meteoric origin, as generated high relief is bordered by oceanic areas, and from deep source, in relation to magmatic and metamorphic processes.

Presently, New Zealand and Philippines are the zones where the exploitation of geothermal energy is the most advanced within these subduction-related contexts.

Collision zones and convergent plate boundaries may also be sites of high geothermal gradients. Collision is responsible for the development of large thrust systems that lead to a crustal thickening of several tens of kilometers. Zones situated at mid-crustal depth within the underthrust slab will then be buried and will undergo an immediate increase in pressure and a progressive increase in temperature. As discussed previously (Figure 1.6), the equilibrium thermal field is reached several ten million years after the thrusting event has ceased. This evolution is

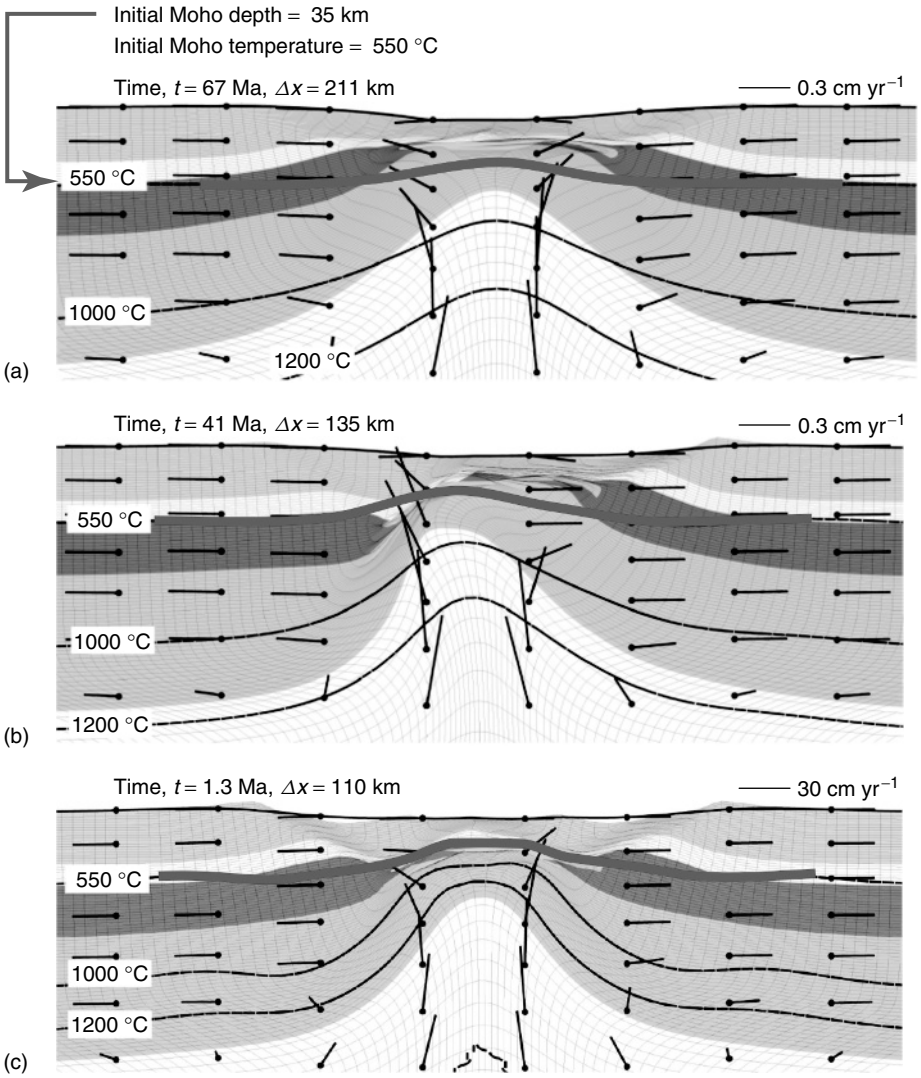

Figure 1.12 Uplifted isotherms (thick grey line) created by lithospheric extension, after Huismans and Beaumont, 2002. Crust and lithosphere are rheologically stratified. Lateral boundary conditions reproducing extension correspond to the imposed rifting velocities given in centimeters per year. (a) Case of no strain softening, after 211 km of extension; (b) asymmetric extension obtained with the introduction of strain softening and 41 Myr after rifting initiation; and (c) case of a fast rifting velocity, involving a large zone (~40 km) of hot middle crust.

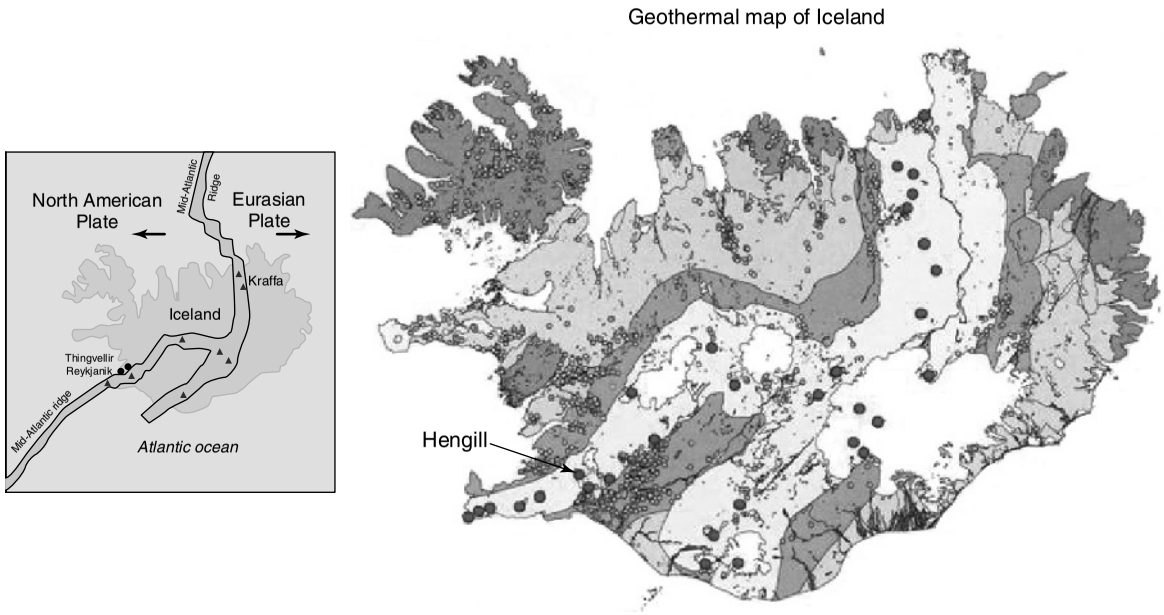

Figure 1.13 Geothermal map of Iceland. The main geothermal fields are located within prehistoric and historic lava centers and interglacial lavas, within the active rift zone.

well documented in the European Variscan belt where high paleogradients determined from mineral assemblages show that a regional geothermal system, responsible for many ore deposits (Au, U, etc.), has been generated during the late orogenic evolution of this collision belt (Bouchot *et al.*, 2005). The melting of large mid-crustal zones has been enhanced by the fertility of the crust rich in radioelements and hydrated minerals generating large volume of migmatites and granites over a long period, from 360 to 300 Ma (Ledru *et al.*, 2001). This situation reflects probably what is occurring within the Tibet Plateau – crustal thickening resulting from the collision between Asia and India being responsible for the development of migmatitic layers at depth. Taking this time delay related to the progressive re-equilibration of the isotherms in the thickened crust, such collision plate boundaries can be considered as favorable zones for high geothermal gradients. Moreover, like in the case of active margins, the concentration of radioelement-rich geological units (differentiated granites, uranium-bearing sedimentary basins, volcanic ash flows, overthrust Precambrian radiogenic granites, etc.) in the upper crust contributes to the thermal budget of the continents over several hundreds of million years.

The location of high geothermal gradients in the vicinity of transform margins and of thermal anomalies along continental-scale strike-slip faults can be related to thickening processes inherited from an early stage of collision, or linked to zones of pull-apart extension (that can be assimilated to the general case of rift systems), or a combination of both processes. In the case of the San Andreas Fault and its satellites in Nevada, it seems that the dominant feature for exploration at the regional scale is the presence of structural discontinuities bordering such pull-apart basins (Figure 1.14, Faulds, Henry, and Hinz, 2005; Faulds *et al.*, 2006).

Within plates, out of these plate boundaries, the lithosphere is considered as stabilized and the main mechanism of heat transfer is conduction. Depending on its composition (i.e., conductivity of its main lithologies) and thickness, geothermal gradients vary between 15 and 25 $^{\circ}$C km^{-1}. The main source of thermal anomalies is the presence of highly radiogenic lithologies such as alkaline and aluminous granites, uranium-bearing sedimentary basins, or highly conductive materials (massive sulfide). The radioactive decay is the cause of heat anomalies in the vicinity and at the apex of these radiogenic bodies, generally of small to medium amplitude and wavelength (Figure 1.5). This is the model on which exploration of deep geothermal resources is done presently in the Southern Australian craton (McLaren *et al.*, 2002; Hillis *et al.*, 2004). Highly radiogenic Precambrian granites ($\sim$16 mW m^{-3}), outcropping in large ranges and found laterally at the base of a Paleozoic sedimentary basins resting unconformably over this basement, are considered as the source of local thermal anomalies that are superposed to a regional anomaly know as the *south Australian heat flow anomaly* (SAHFA) (McLaren *et al.*, 2003; Chopra and Holgate, 2005). Paralana hot springs are observed along the main faulted contact between the basement and cover sequences and uranium-bearing sediments deposited during the erosion of the radiogenic Precambrian granites are presently exploited by *in situ* recovery (Berveley mine). The company Petratherm

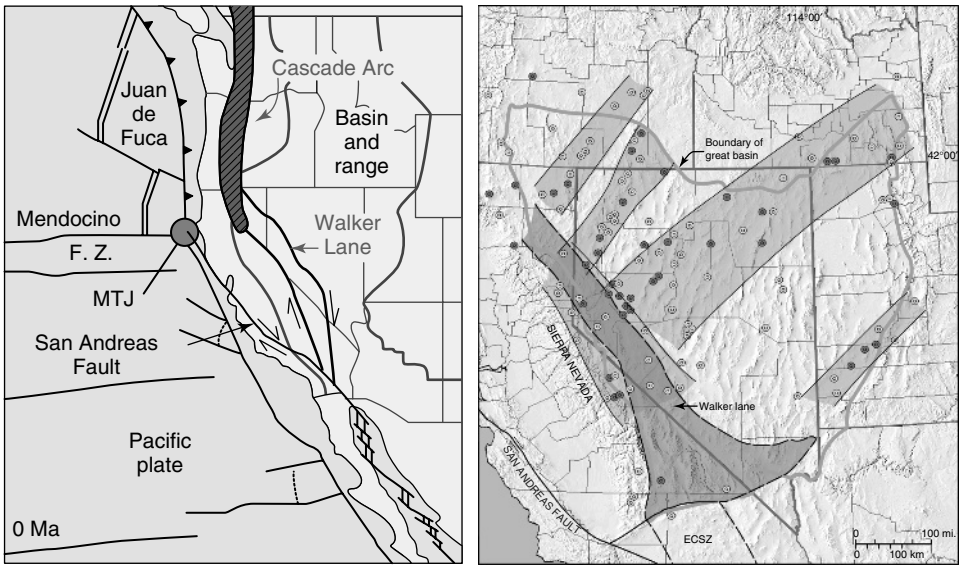

Figure 1.14 Geothermal fields in the Great Basin, western United States. Most of the activity is concentrated in the transtensional northwestern Great Basin within NE-trending belts oriented orthogonal to the extension direction and radiating from the northwestern terminus of the Walker Lane dextral shear zone (dark grey). Black spots, high temperature geothermal systems (>160 °C); open circles, low temperature systems (<160 °C); ECSZ, eastern California shear zone.

has drilled on Paralana 1B down to 1.8 km, which suggests 200 °C at 3.6 km, that is, more than 50 °C km^{-1}. In that case, the reservoir should be the Infracambrian detrital sedimentary sequences.

1.3.2
Porosity, Permeability, and Fluid Flow in Relation to the Stress Field

The permeability of the continental crust is defined by the capacity of the geological medium to transmit fluid. It constitutes a critical geological parameter for the definition of the geothermal reservoir as it plays a fundamental role in heat and mass transfer (Manning and Ingebritsen, 1999). This parameter is related to two basic properties of the rocks:

1) The porosity is the ratio of pore volume to the total volume. The intrinsic permeability is the measure of the fluid flow through the pore network of the rock and will be directly correlated to the porosity. These parameters are directly linked to the packing of the minerals within the rocks, which is a result of the nature, size, sorting of the minerals and elements, and of the compaction and diagenetic history. Sedimentary rocks such as limestone, sandstone, or

conglomerate are generally porous and can store large quantities of fluids within their pore network. They constitute natural reservoirs in the crust for all kind of fluids. The intrinsic permeability parameter is the primary control on fluid flow as it will vary from 10^{-23} m^2 in intact crystalline rocks to 10^{-7} m^2 in detrital porous sediments; meaning 16 orders of magnitude variations (Manning and Ingebritsen, 1999).

2) The fracture permeability is linked to the discontinuities that are present within the rock along which fluid circulation is possible. This type of permeability is generally well developed in crystalline massifs. Thus, although granite is a nonpermeable rock, a granitic massif will be considered as a permeable massif as a whole – fluid circulating along the fracture network. Implicitly, such permeability will be well developed in the vicinity of large fracture systems, whether active or fossil. Because of the discontinuous character of the fracture and their geometrical complexity, the intrinsic permeability of such system is more difficult to evaluate compared to stratified permeable layers.

The range of permeability observed and measured in the continental crust can be illustrated by a one-dimensional graph (Figure 1.15). Geothermal reservoirs are characterized by rather large permeability, higher than 10^{-13} m^2. Analyses of coupled groundwater flow and heat transport in the upper crust infer permeabilities in the range of 10^{-17}–10^{-14} m^2 with a mean value greater than 10^{-16} m^2 (Manning and Ingebritsen, 1999).

The identification of potential geothermal reservoir will then focus in priority on the exploration of both types of permeability related to the intrinsic and fracture permeability properties. A good knowledge of the geometry of the geological units and their physical properties, determined *in situ* or by geophysical methods, and of the structural pattern is a key for successful exploration. The building of a 3D

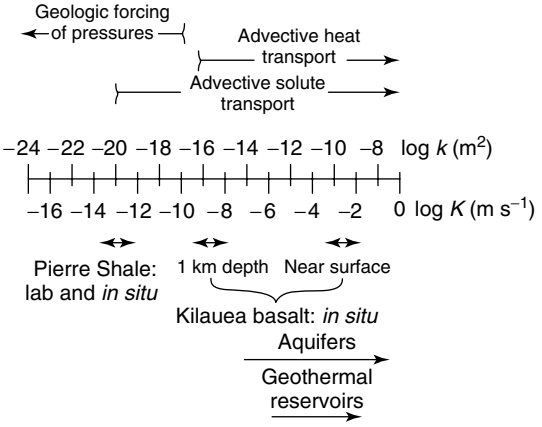

Figure 1.15 Range of permeabilities observed in geologic media: permeability (k, m^2) and hydraulic conductivity ($K = k\rho fg/\mu$, m s^{-1}) in relation to water density ρ_w and viscosity μ_w at 15 °C.

geometric model and the realization of 2D or even 3D seismic surveys are presently strategies that are promoted by many exploration companies, such as ENEL in Larderello or in the Rhine graben.

The main source of fluids is water in the ocean and meteoric water in the continents. The infiltrated part of meteoric and sea water will migrate down within permeable lithologies and/or fracture systems. Depending of the tectonic sites and of the geothermal gradient, they will be heated to temperature that will already be sufficient for direct use or even power generation. This is the case of the basin located in thinned crust such as the Rhine graben. What is the lower boundary of this infiltration?

Besides the first-order variation related to the intrinsic permeability of the systems, variation of permeability is also recorded with depth. Permeability of fractured crystalline rocks decreases with increasing pressure or effective stress. The porosity will be also controlled by the pressure–temperature conditions, and an increase in pressure with depth will reduce the porosity as the compaction will be greater. Surveys performed during deep drilling programs have demonstrated this decreasing permeability at depth, between 10^{-17} and 10^{-15} m^2 above 4 km depth and 10^{-18}–10^{-16} m^2 below (Huenges *et al.*, 1997), and a paper on the variation of permeability as a function of depth based on geothermal data and metamorphic systems was published in 1999 by Manning and Ingebritsen (Figure 1.16). With respect to this aspect, the brittle–ductile transition is a major decoupling surface at the scale of the crust that marks the lower limit that meteoric water can reach at depth and a change in fluid flow processes as it has been shown in natural analog (Famin *et al.*, 2004).

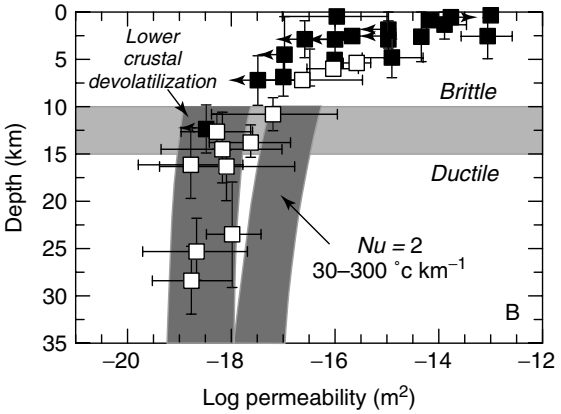

Figure 1.16 Permeability as a function of depth in the continental crust based on geothermal data (solid squares) and metamorphic systems (open squares). (After Manning and Ingebritsen, 1999)

.

If the intrinsic permeability of the continental crust is low below the brittle–ductile transition zones, fluid flow will occur through pervasive flow in zones of low strain rates and homogeneous lithologies while higher strains and a more heterogeneous rheology will favor a channeled flow (Oliver, 1996). In the case of the geothermal reservoirs, attention will be paid on the channeled flow that will occur along active tectonic zones or on emplacement of magmatic or volcanic suites. In such environments, hot fluids with temperature generally greater than 250 °C will move upward and finally reach the surface if they are not trapped by a cap nonpermeable layer or blocked within the fracture network. They ascend through the crust and will get connected, at the brittle–ductile transition zone, with fluids that have been infiltrated from surface. Many of the active geothermal fields are in fact resulting from the mixing between these ascending and descending fluids within the permeability network of the continental crust. A loop is created at the level of the reservoir, corresponding to a convective transfer of heat toward surface. Geysers from Iceland or from western United States are the most visible trace of this phenomenon.

This link between the permeability of the continental crust, the potential infiltration of meteoric fluids and seawater, the brittle–ductile transition at depth, and the potential connection to fluid of deep origin illustrates the need to have a global approach for the exploration of geothermal reservoirs. Thus, numerous studies dedicated to tectonic processes during prograde and retrograde metamorphism or to transfer and trapping of hydrothermal ore deposits could provide a lot of information about the variation of permeability in the continental crust.

Other variations of permeability are observed laterally within one single geological medium depending on heterogeneity, anisotropy, and time. These parameters constrain the efficiency of the reservoir and its sustainable use. The intrinsic permeability is a function of the heterogeneity and anisotropy of the medium. Fluid flow will tend to be greater parallel to the main layering of the sedimentary or volcanic rocks and foliation of metamorphic rocks rather than across them. Permeability is also a time-dependent process as fluid–rock interactions will provoke permanent dissolution and recrystallization phenomenon that will modify the permeability network. The intensity and orientation of the stress field will exert a direct control on this process by determining zones of compression and extension, in relation to the relative position of the main stress axis and resulting strain.

1.3.3 Summary

The review of the phenomena that control the distribution of heat and fluid at depth shows that conventional reservoirs for high enthalpy geothermal energy are located in zones of active volcanism or magmatism while low- to medium enthalpy can be found in varied environment. The identification of potential reservoirs for developing a heat exchanger is linked to our ability to evaluate the coincidence

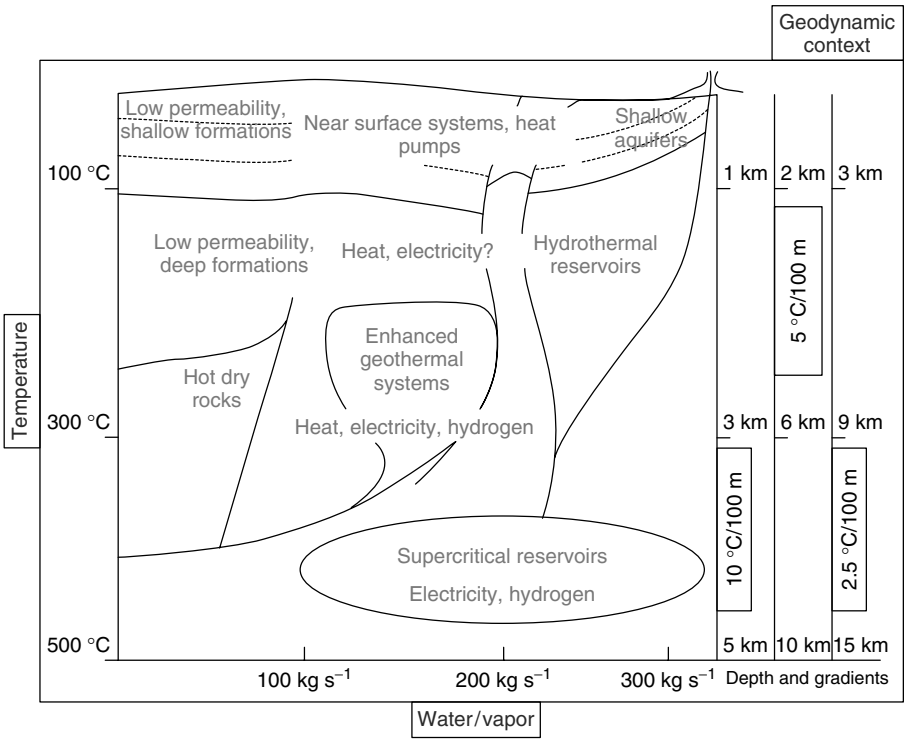

Figure 1.17 Sketch section showing the variety of reservoirs that can be used for heat extraction and the different uses of the geothermal energy.

of the following four independent parameters: heat, fluid flow, permeability, and appropriate orientation of the stress field in relation to the permeability network. Among these parameters, only fluid flow and permeability can be enhanced by engineering. These parameters are summarized in one sketch section that illustrates the variety of reservoirs that can be used for heat extraction and the various uses of the geothermal energy (Figure 1.17).

Following chapters will analyze the different processes of stimulation that can be applied for achieving such improvement. Lessons learned from the Soultz EGS experiment, the sustainable development of the Larderello field in Italy, and the Icelandic geothermal power network, among other case histories, show that the concept of geothermal reservoir must not be too restricted. Experiences of stimulation can be realized by extending active geothermal fields and the development of binary plants makes possible the exploitation of geothermal reservoirs with minimum temperatures of 85–100 °C for power generation.

A reservoir is also defined by its economic viability. Many other parameters such as the price of the steel involved in drilling, cost of drilling depending on the

availability of drilling companies active on the "exploration market," and feed in tariffs supporting the development of geothermal energy must then be taken into account to evaluate the feasibility and viability of the project. These questions will be reviewed in the following chapters.

References

Arnórsson, S. (1995) Geothermal systems in Iceland: structure and conceptual models – I. High-temperature areas. *Geothermics*, **24**, 561–602.

Aydin, I., Karat, H.I., and Kocak, A. (2005) Curie-point depth map of Turkey. *Geophysical Journal International*, **162**, 633–640.

Bächler, D., Kohl, T., and Rybach, L. (2003) Impact of graben-parallel faults on hydrothermal convection – Rhine graben case study. *Physics and Chemistry of the Earth*, **28**, 431–441.

Beziat, A., Dardaine, M., and Gabis, V. (1988) Effect of compaction pressure and water content on the thermal conductivity of some natural clays. *Clay and Clay Minerals*, **36**, 462–466.

Blackwell, D.D., Steele, J.L., and Brott, C.A. (1980) The terrain effect on terrestrial heat flow. *Journal of Geophysical Research*, **85**, 4757–4772.

Bonté, D., Guillou-Frottier, L., Garibaldi, C., Lopez, S., Bourgine, B., Lucazeau, F., and Bouchot, V. (2010) Subsurface temperature maps in French sedimentary basins: new data compilation and interpolation. Submitted to *Bulletin de la Société Géologique de France in press*.

Bouchot, V., Ledru, P., Lerouge, C., Lescuyer, J.L., and Milesi, J.P. (2005) Late Variscan mineralizing systems related to orogenic processes: the French Massif Central. *Ore Geology Reviews*, **27**, 169–197.

Burov, E., Jaupart, C., and Guillou-Frottier, L. (2003) Ascent and emplacement of buoyant magma bodies in brittle-ductile upper crust. *Journal of Geophysical Research*, **108** (B4), 2177. doi: 10.1029/2002JB001904.

Cagnioncle, A.M., Parmentier, E.M., and Elkins-Tanton, L. (2007) Effect of solid flow above a subducting slab on water distribution and melting at convergent plate boundaries. *Journal of Geophysical Research*, **112**. doi: 10.1029/2007JB004934.

Cathles, L.M. (1977) An analysis of the cooling of intrusives by ground water convection which includes boiling. *Economic Geology*, **72**, 804–826.

Cermak, V. (1993) Lithospheric thermal regimes in Europe. *Physics of the Earth and Planetary Interiors*, **79**, 179–193.

Cermak, V., Kresl, M., Kucerova, L., Safanda, J., Frasheri, A., Kapedani, N., Lico, R., and Cano, D. (1996) Heat flow in Albania. *Geothermics*, **25**, 91–102.

Chopra, P. and Holgate, F. (2005) A GIS analysis of temperature in the Australian crust. Proceedings World Geothermal Congress 2005, April 24-29, 2005, Antalya, Turkey.

Clauser, C. (2006) Geothermal energy, in *Landolt-Börnstein, Group VIII: Advanced Materials and Technologies*, Energy Technologies, Subvol. C: Renewable Energies, Vol. **3** (ed K.Heinloth), Springer-Verlag, Heidelberg, Berlin, pp. 493–604.

Clauser, C. and Huenges, E. (1995) Thermal conductivity of rocks and minerals, in *Rock Physics and Phase Relations: A Handbook of Physical Constants*, AGU Reference Shelf, Vol. **3** (ed T.J. Ahrens), AGU, Washington, DC, pp. 105–126.

Delescluse, M. and Chamot-Rooke, N. (2008) Serpentinization pulse in the actively deforming central Indian basin. *Earth and Planetary Science Letters*, **276**, 140–151.

Demetrescu, C. and Andreescu, M. (1994) On the thermal regime of some tectonic units in a continental collision environment in Romania. *Tectonophysics*, **230**, 265–276.

Demongodin, L., Pinoteau, B., Vasseur, G., and Gable, R. (1991) Thermal conductivity and well-logs – a case study in the Paris basin. *Geophysical Journal International*, **105**, 675–691.

Dèzes, P., Schmid, S.M., and Ziegler, P.A. (2004) Evolution of the European Cenozoic Rift System: interaction of the Alpine

and Pyrenean orogens with their foreland lithosphere. *Tectonophysics*, **389**, 1–33.

Dini, A., Gianelli, G., Puxeddu, M., and Ruggieri, G. (2004) Origin and evolution of Pliocene–Pleistocene granites from the Larderello geothermal field (Tuscan Magmatic Province, Italy). *Lithos*, **81**, 1–31.

Drury, M.J., Jessop, A.M., and Lewis, T.J. (1984) The detection of groundwater flow by precise temperature measurements in boreholes. *Geothermics*, **13**, 163–174.

Edel, J.B. and Fluck, P. (1989) The upper Rhenish shield basement (Vosges, Upper Rhinegraben and Schwarzwald): main structural features deduced from magnetic, gravimetric and geological data. *Tectonophysics*, **169**, 303–316.

Elder, J. (1967) Convective self-propulsion of continents. *Nature*, **214**, 657–660.

Elder, J. (1981) *Geothermal Systems*, Academic Press, London, 508 pp.

Emmanuel, S. and Berkowicz, B. (2006) An experimental analogue for convection and phase separation in hydrothermal systems. *Journal of Geophysical Research*, **111**, B09103. doi: 10.1029/2006JB004351.

England, P.C. and Thompson, A.B. (1984) Pressure-temperature-time paths of regional metamorphism. 1. Heat transfer during the evolution of regions of thickened continental crust, *Journal of Petrology*, **25**, 894–928.

Ercan, A. (2002) Petroleum and geothermal model of Aegean Sea and western Anatolia. *Turkey: Second Balkan Geophysical Congress and Exhibition*, 158–159.

Famin, V., Philippot, P., Jolivet, L. and Agard, P. (2004) Evolution of hydrothermal regime along a crustal shear zone, Tinos Island, Greece. *Tectonics*, **23**, TC5004. doi: 10.1029/2003TC001509.

Faulds, J.E., Coolbaugh, M.F., Vice, G.S., and Edwards, M.L. (2006) Characterizing structural controls of geothermal fields in the northwestern great basin: a progress report: *Geothermal Resources Council Transactions*, **30**, 69–76.

Faulds, J.E., Henry, C.D., and Hinz, N.H. (2005) Kinematics of the northern Walker Lane: an incipient transform fault along the Pacific –North American plate boundary. *Geology*, **33**, 505–508.

Fernàndez, A., Marzán, I., Correia, A., and Ramalho, E. (1998) Heat flow, heat production, and lithospheric thermal regime in the Iberian Peninsula. *Tectonophysics*, **291**, 29–53.

Flóvenz, O. and Saemundsson, K. (1993) Heat flow and geothermal processes in Iceland. *Tectonophysics*, **225**, 123–138.

Gallagher, K., Ramsdale, M., Lonergan, L., and Morrow, D. (1997) The role of thermal conductivity measurements in modelling thermal histories in sedimentary basins. *Marine and Petroleum Geology*, **14**, 201–214.

Garibaldi, C., Guillou-Frottier, L., Lardeaux, J.M., Bonté, D., Lopez, S., Bouchot, V. and Ledru, P. (2010) Relationship between thermal anomalies, geological structures and fluid flow: new evidence in application to the Provence basin (south-east France). Submitted to *Bulletin de la Société Géologique de France in press*.

Genter, A., Guillou-Frottier, L., Feybesse, J.-L., Nicol, N., Dezayes, C., and Schwartz, S. (2003) Typology of hot fractured rock resources in Europe. *Geothermics*, **32**, 701–710.

Goes, S., Loohuis, J.J.P., Wortel, M.J.R., and Govers, R. (2000) The effect of plate stresses and shallow mantle temperatures on tectonics of northwestern Europe. *Global and Planetary Change*, **27**, 23–38.

Goes, S., Spakman, W., and Bijwaard, H. (1999) A lower mantle source for central European volcanism. *Science*, **286**, 1928–1931.

Goutorbe, B., Lucazeau, F., and Bonneville, A. (2007) Comparison of several BHT correction methods: a case study of an Australian data set. *Geophysical Journal International*, **170**, 913–922.

Granet, M., Wilson, M., and Achauer, U. (1995) Imaging a mantle plume beneath the French Massif Central. *Earth and Planetary Science Letters*, **136**, 281–296.

Grigné, C. and Labrosse, S. (2001) Effects of continents on Earth cooling: thermal blanketing and depletion in radioactive elements. *Geophysical Research Letters*, **28**, 2707–2710.

Guillou, L. and Jaupart, C. (1995) On the effect of continents on mantle convection. *Journal of Geophysical Research*, **100**, 24217–24238.

Guillou, L., Mareschal, J.-C., Jaupart, C., Gariépy, C., Bienfait, G., and Lapointe, R. (1994) Heat flow, gravity and structure of the Abitibi belt, Superior Province, Canada: implications for mantle heat flow. *Earth and Planetary Science Letters*, **122**, 103–123.

Guillou-Frottier, L., Burov, E., Nehlig, P., and Wyns, R. (2007) Deciphering plume-lithosphere interactions beneath Europe from topographic signatures. *Global and Planetary Change*, **58**, 119–140.

Guillou-Frottier, L., Mareschal, J.-C., Jaupart, C., Gariépy, C., Lapointe, R., and Bienfait, G. (1995) Heat flow variations in the Grenville Province, Canada. *Earth and Planetary Science Letters*, **136**, 447–460.

Guillou-Frottier, L., Mareschal, J.-C., and Musset, J. (1998) Ground surface temperature history in central Canada inferred from ten selected borehole temperature profiles. *Journal of Geophysical Research*, **103**, 7385–7397.

Gurnis, M. (1988) Large-scale mantle convection and the aggregation and dispersal of supercontinents. *Nature*, **332**, 695–699.

Haenel, R. and 16 co-authors (1980) Atlas of Subsurface Temperatures in the European Community, The Commission of the European Communities, 36 p., 43 plates.

Hansen, J. and Lebedeff, S. (1987) Global trends of measured surface air temperatures. *Journal of Geophysical Research*, **92**, 13345–13372.

Harcouët, V., Guillou-Frottier, L., Bonneville, A., Bouchot, V., and Milesi, J.-P. (2007) Geological and thermal conditions before the major Paleoproterozoic gold mineralization event at Ashanti, Ghana, as inferred from improved thermal modelling. *Precambrian Research*, **154**, 71–87.

Hillis, R.R., Hand, M., Mildren, S., Morton, J., Reid, P., and Reynolds, S. (2004) Hot dry rock geothermal exploration in Australia, application of the in situ stress field to hot dry rock geothermal energy in the Cooper Basin. Eastern Australian Basins Symposium II Volume. Petroleum Exploration Society of Australia (PESA) Eastern Australian Basins Symposium, Adelaide, pp. 413–421.

Huenges, E., Erzinger, J., Kuck, J., Engeser, B., and Kessels, W. (1997) The permeable crust: geohydraulic properties down to 9101 m depth. *Journal of Geophysical Research*, **102**, 18,255–18,265.

Huismans, R.S. and Beaumont, C.B. (2002) Asymmetric lithospheric extension: the role of frictional plastic strain softening inferred from numerical experiments. *Geology*, **30**, 211–214.

Huismans, R.S., Podladchikov, Y.Y., and Cloetingh, S. (2001) Dynamic modeling of the transition from passive to active rifting: application to the Pannonian basin. *Tectonics*, **20**, 1021–1039.

Hurtig, E., Cermak, V., Haenel, R., and Zui, V. (eds) (1992) *Geothermal Atlas of Europe*, Hermann Haack Verlagsgesellschaft mbH, Germany.

Jaupart, C., Labrosse, S., and Mareschal, J.-C. (2007) Elsevier, Temperatures, heat and energy in the mantle of the Earth, in *Treatise on Geophysics*, Mantle Dynamics, Vol. **7** (eds D. Bercovici and G. Schubert), pp. 253–303.

Jaupart, C., Mareschal, J.-C., Guillou-Frottier, L., and Davaille, A. (1998) Heat flow and thickness of the lithosphere in the Canadian Shield. *Journal of Geophysical Research*, **103**, 15269–15286.

Jaupart, C. and Parsons, B. (1985) Convective instabilities in a variable viscosity fluid cooled from above. *Physics of the Earth and Planetary Interiors*, **39**, 14–32.

Kukkonen, I.T. and Peltonen, P. (1999) Xenolith-controlled geotherm for the central Fennoscandian Shield: implications for lithosphere-asthenosphere relations. *Tectonophysics*, **304**, 301–315.

Labrosse, S. (2002) Hotspots, mantle plumes and core heat loss. *Earth and Planetary Science Letters*, **199**, 147–156.

Ledru, P., Courrioux, G., Dallain, C., Lardeaux, J.M., Montel, J.M., Vanderhaeghe, O., and Vitel, G. (2001) The Velay dome (French Massif Central): melt generation and granite emplacement during orogenic evolution. *Tectonophysics*, **342**, 207–227.

Lenardic, A., Guillou-Frottier, L., Mareschal, J.-C., Jaupart, C., Moresi, L.-N., and Kaula, W.M. (2000) Amer. Geophys. Union, What the mantle sees: the effects of continents on mantle heat flow, in *The History and Dynamics of Global Plate Motions*, AGU Monograph, Vol. **121** (eds M. Richards *et al.*), pp. 95–112.

Lenardic, A. and Kaula, W.M. (1995) Mantle dynamics and the heat flow into the Earth's continents. *Nature*, **378**, 709–711.

Lister, C.R.B., Sclater, J.G., Davis, E.E., Villinger, H., and Nagahira, S. (1990) Heat flow maintained in ocean basins of great age: investigations in the north equatorial west Pacific. *Geophysical Journalal*, **102**, 603–630.

Lopez, D. and Smith, L. (1995) Fluid flow in fault zones: analysis of the interplay of convective circulation and topographically driven groundwater flow. *Water Resources Research*, **31**, 1489–1503.

Lucazeau, F. and 10 co-authors (2008) Persistent thermal activity at the eastern Gulf of Aden after continental break-up. *Nature Geosciences*, **1**, 854–858.

Lucazeau, F., Vasseur, G., and Bayer, R. (1984) Interpretation of heat flow data in the French Massif Central. *Tectonophysics*, **103**, 99–119.

Manea, V.C., Manea, M., Kostoglodov, V., Currie, C.A., and Sewell, G. (2004) Thermal structure, coupling and metamorphism in the Mexican subduction zone beneath Guerrero. *Geophysical Journal International*. **158**, 775–784.

Manning, C.E. and Ingebritsen, S.E. (1999) Permeability of the continental crust: implications of geothermal data and metamorphic systems. *Review of Geophysics*, **37**, 127–150.

Mareschal, J.-C., Jaupart, C., Gariépy, C., Cheng, L.Z., Guillou-Frottier, L., Bienfait, G., and Lapointe, R. (2000) Heat flow and deep thermal structure near southeastern edge of the Canadian Schield. *Canadian Journal of Earth Sciences*, **37**, 399–414.

McLaren, S., Dunlap, W.J., Sandiford, M., and McDougall, I. (2002) Thermochronology of high heat-producing crust at Mount Painter, South Australia: implications for tectonic reactivation of continental interiors. *Tectonics*, **21**. doi: 10.1029/2000TC001275.

McLaren, S.N., Sandiford, M., Hand, M., Neumann, N.L., Wyborn, L.A.I., and Bastrakova, I. (2003) The hot southern continent: heat flow and heat production in Australian Proterozoic terranes, in *Evolution and Dynamics of the Australian Plate* (eds R.R. Hillis and R.D. Müller), Geological Society of Australia Special Publication 22 and Geological Society of America Special Paper 372, pp. 157–167.

Mwenifumbo, C.J. (1993) Temperature logging in mineral exploration. *Journal of Applied Geophysics*, **30**, 297–313.

Nemcock, M., Pospisil, L., Lexa, J., and Donelick, R.A. (1998) Tertiary subduction and slab break-off model of the Carpathian-pannonian region. *Tectonophysics*, **295**, 307–340.

Norton, D.L. and Hulen, J.B. (2001) Preliminary numerical analysis of the magma-hydrothermal history of The Geysers geothermal system, California, USA. *Geothermics*, **30**, 211–234.

Oliver, N.H.S. (1996) Review and classification of structural controls on fluid flow during regional metamorphism. *Journal of Metamorphic Geology*, **14**, 447–492.

Parsons, B. and McKenzie, D. (1978) Mantle convection and the thermal structure of plates. *Journal of Geophysical Research*, **83**, 4485–4496.

Parsons, B. and Sclater, J.G. (1977) An analysis of the variation of ocean floor bathymetry and heat flow with age. *Journal of Geophysical Research*, **82**, 803–827.

Peacock, S.M., van Keken, P.E., Holloway, S.D., Hacker, B.R., Abers, G.A., and Fergason, R.L. (2005) Thermal structure of the Costa Rica – Nicaragua subduction zone. *Physics of the Earth and Planetary Interiors*, **149**, 187–200.

Pinet, C., Jaupart, C., Mareschal, J.-C., Gariépy, C., Bienfait, G., and Lapointe, R. (1991) Heat flow and structure of the lithosphere in the eastern Canadian Schield. *Journal of Geophysical Research*, **96**, 19941–19963.

Pollack, H.N., Hurter, S.J., and Johnson, J.R. (1993) Heat flow from the Earth's interior: analysis of the global data set. *Review of Geophysics*, **31**, 267–280.

Pribnow, D. and Schellschmidt, R. (2000) Thermal tracking of upper crustal fluid flow in the Rhine graben. *Geophysical Research Letters*, **27**, 1957–1960.

Ritter, J.R.R., Jordan, M., Christensen, U.R., and Achauer, U. (2001) A mantle plume below the Eifel volcanic fields, Germany. *Earth and Planetary Science Letters*, **186**, 7–14.

Roberts, P.H., Jones, C.A., and Calderwood, R.A. (2003) Energy fluxes and ohmic dissipation in the Earth's core, in *Earth's Core and Lower Mantle* (eds C.A. Jones, A.M. Soward, and K. Zhang), Taylor and Francis, London, pp. 100–129.

Rühaak, W. (2009) Multidimensional modeling of the thermal and flow regime in the western part of the Molasse Basin, Southern Germany, PhD thesis, University of Aachen, Germany, 88 p.

Ruppel, C. and Hodges, K. (1994) Role of horizontal thermal conduction and finite time thrust emplacement in simulation of pressure-temperature-tile paths. *Earth and Planetary Science Letters*, **123**, 49–60.

Sandiford, M., Fredericksen, S., and Braun, J. (2003) The long term thermal consequences of rifting: implications for basin reactivation. *Basin Research*, **15**, 23–43.

Sandiford, M., McLaren, S., and Neumann, N. (2002) Long-term thermal consequences of the redistribution of heat-producing elements associated with large-scale granitic complexes. *Journal of Metamorphic Geology*, **80**, 87–98.

Schubert, G., Turcotte, D.L., and Olson, P. (2002) *Mantle Convection in the Earth and Planets*, Cambridge University Press, 956 p.

Sclater, J.G., Jaupart, C., and Galson, D.A. (1980) The heat flow through oceanic and continental crust and the heat loss of the Earth. *Review of Geophysics*, **18**, 269–311.

Sengör, A.M.C., Gorur, N., and Saroglu, F. (1985) Strike-slip faulting and related basin formation in zones of tectonic escape: Turkey as a case study, in *Strike-slip Faulting and Basin Formation*, Special Publication 37 (eds K.T. Biddle and N. Christie-Black), Society of Economic, Paleontologic, and Mineralogists, pp. 227–264.

Shapiro, N.M. and Ritzwoller, M.H. (2002) Monte-Carlo inversion for a global shear-velocity model of the crust and upper mantle. *Geophysical Journal International*, **151**, 88–105.

Sonney, R. and Vuataz, F.D. (2008) Properties of geothermal fluids in Switzerland: a new interactive database. *Geothermics*, **37**, 496–509.

Trubitsyn, V., Kaban, M., Mooney, W., Reigber, C., and Schwintzer, P. (2006) Simulation of active tectonic processes for a convecting mantle with moving continents. *Geophysical Journal International*, **164**, 611–623.

Turcotte, D.L. and Schubert, G. (2002) *Geodynamics*, 2nd edn, Cambridge University Press, 450 p.

Vasseur, G., Brigaud, F., and Demongodin, L. (1995) Thermal conductivity estimation in sedimentary basins. *Tectonophysics*, **244**, 167–174.

Vasseur, G., Gable, R., Feuga, B., and Bienfait, G. (1991) Groundwater flow and heat flow in an area of mineral springs. *Geothermics*, **20**, 99–117.

Waples, D.W. and Tirsgaard, H. (2002) Changes in matrix thermal conductivity of clays and claystones as a function of compaction. *Petroleum Geoscience*, **8**, 365–370.

Wenzel, F. and Brun, J.-P., ECORS-DEKORP Working Group (1991) A deep reflection seismic line across the Northern Rhine Graben. *Earth and Planetary Science Letters*, **104**, 140–150.

Whitehead, J.A. (1976) Convection models: laboratory versus mantle. *Tectonophysics*, **35**, 215–228.

Wisian, K.W. and Blackwell, D.D. (2004) Numerical modeling of Basin and Range geothermal systems. *Geothermics*, **33**, 713–741.